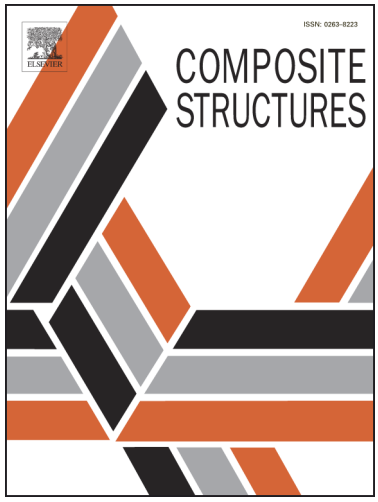

Two-steps clinching of Aluminum and Carbon Fiber Reinforced Polymer Sheets

Francesco Lambiase, Dae-Cheol Ko

PII: S0263-8223(16)32319-4
DOI: http://dx.doi.org/10.1016/j.compstruct.2016.12.072
Reference: COST 8127

To appear in: *Composite Structures*

Received Date: 27 October 2016
Revised Date: 12 December 2016
Accepted Date: 27 December 2016

Please cite this article as: Lambiase, F., Ko, D-C., Two-steps clinching of Aluminum and Carbon Fiber Reinforced Polymer Sheets, *Composite Structures* (2016), doi: http://dx.doi.org/10.1016/j.compstruct.2016.12.072

Two-steps clinching of Aluminum and Carbon Fiber Reinforced Polymer Sheets

Francesco Lambiase[1,2] and Dae-Cheol Ko[3]

[1]Dept. of Industrial and Information Engineering and Economics, University of L'Aquila, via G. Gronchi 18, Zona Industriale di Pile, 67100 (AQ), Italy.
[2]University of Naples Federico II, CIRTIBS Research Centre, P.le Tecchio 80, 80125 Naples, Italy.
[3]Graduate School of Convergence Science, Pusan National University, Busan, 46241, South Korea.

Abstract

The present paper investigates the effectiveness of two-steps clinching for joining aluminum and Carbon Fiber Reinforced Polymer (CFRP). To this end, different reshaping tools were involved after joining by clinching with split dies. The reshaping force was also varied. Single lap shear tests of simple clinched and reshaped specimens were performed to determine the influence of the process conditions on the mechanical behavior of the joints. The morphology and geometry of joints were analyzed to understand how the reshaping step influences the main quality criteria of the joints and the damage produced on the CFRP sheet. According to the experimental results, simple clinched connection failed by pullout; thus, the critical parameter was the undercut. The reshaping method, using optimized tools enabled to increase the strength of the joints by 32%. Such an improvement was due to an increase in the undercut that resulted from a higher and improved material flow. The main defects that may appear in these joints have been identified as well as their causes.

Keywords: joining; metal; clinching; CFRP; hybrid joints; composite.

[1] Corresponding author:
F. Lambiase
francesco.lambiase@univaq.it
Monteluco di Roio, 67040 (AQ), Italy
Tel. N.: (+39) 0862 434343
Fax N.: (+39) 0862 434303

1. Introduction

Hybrid metal-composite structures are more and more employed in several fields including transportation industries, civil infrastructure and construction as they enable great reduction in product weight, fuel savings, inertia reduction (and thus higher performances). Automotive industries are investing high efforts to reproduce on larger scale the benefits of using hybrid metal-composite chassis. In recent years, such chassis are being employed on a number of vehicles of mass production, including Alfa Romeo 4C, BMW 7-series and Chevrolet Corvette Z06. Hybrid metal-composite structures are also widely employed in civil applications with different scopes: reinforcing bridge constructions [1], increasing flexural rigidity of aluminum beams [2], repairing and strengthening structural components [3] and even protecting from fire and thermally insulating lightweight structural materials [4].

Because of the great difference, joining such materials still represents a challenging issue and it is generally made by means of adhesive bonding and mechanical joining processes. Compared to adhesive bonds, mechanical joints generally ensure higher static and dynamic load capacity. In addition, these joints are performed in shorter time because they do not require extensive surface preparation (including etching, grinding, and degreasing), is environmentally friendly (due to low energy requirements, low-noise and fumes emission) and do not require curing time. However, mechanical joining processes usually require preliminary drilling of the sheets that may damage the composite material, cause fiber interruption, and produce stress concentration. Although they require shorter time as compared to adhesive bonding, mechanical joining processes involve manual steps such as predrilling and subsequent insertion of extra joining elements and require additional material (rivets, bolts, etc.) that increase the production time, costs, and structure weight.

Despite of mechanical joints, adhesive bonding enables ensuring the integrity of the composite part (no fibers interruption is produced) and the load is distributed more uniformly since the absence of holes [5]. In this case, the stress is almost uniform in width direction while it follows a “U” shape distribution along the bonding length [6]. In these joints, the debonding generally initiates at or near one of the bond extremities [7].

Coupling mechanical joining and adhesive bonding leading to hybrid joints represents an interesting improvement, since it brings together the advantages of both these joining technologies. Hybrid joining has proven to improve both the static [8] and fatigue strength [9], due to lower stress concentration developing during service life. Because of the large variety of mechanical joining processes, different mechanical connections can be coupled with adhesive bonding, including: bolted [8], riveted [10], laser riveting, and self-pierce rivets [11].

Since the increasing employment of hybrid structures for mass productions, faster joining processes are required. A number of new processes have been developed to join fiber-reinforced thermoplastics: friction spot joining [12], friction lap welding, [13], ultrasonic welding [14], and laser-assisted direct joining [15]. These processes produce mechanical and chemical adhesion between the thermoplastic matrix of the composite and the metal surface. In addition, advanced thermoforming processes, which produce a mechanical interlock between the components by plastically deforming the composite are also suitable for this purpose. Thermoforming processes include: friction-based stacking [16], infrared stacking [17], friction riveting [18], and flow drilling [19]. Nevertheless, these processes are not suitable for joining composites with thermosetting matrices, since they would produce thermal degradation of the polymer and mechanical damage of both the fiber and the matrix, tearing of the fibers, and delamination of the composite.

On the other hand, fast mechanical joining processes such as clinching [20-26] and self-pierce riveting [27-29] enable to overcome some of the abovementioned concerns. Indeed, despite of common mechanical joining methods, which involve rivets and bolts, both these processes do not require preliminary drilling of a hole in the sheets being joined [30, 31]. In addition, clinching enables additional advantages, as it does not require external joining elements, which involve higher costs as well as increase the structure weight.

Mechanical clinching consists in the formation of an undercut that fastens two or more sheets. The undercut is produced by a plastic deformation by using a punch and a die. Clinching has been originally developed to join metal sheets including high strength steels and aluminum alloys. Then, it has been extended to join advanced metals (magnesium and titanium alloys), as well as thermoplastic polymers [32], wood materials [33] and also composites sheets with Fiber Reinforced Polymer (FRP) with thermoplastic matrix and short fibers [34] and thermosetting matrix [35] with long fibers.

The proper design of the clinching tools is aimed at increasing the main joint quality parameters (the undercut and the neck thickness), without damaging the sheets [36]. Mechanical clinching of composites introduces further concerns since delamination of the composite should be also limited or possibly avoided.

Thus, specific configurations such as hole clinching has been proposed [37], which consists in preliminary drilling of the composite. However, hole clinching introduces further concerns such as longer processing times (owing to the predrilling operation), and eccentricity between the punch and the hole [38]. Furthermore, during hole clinching, the punch-sided sheet is subjected to higher tearing stress that may compromise the integrity of the sheets for materials with poor formability [39]. As above-mentioned, the mechanical behavior of clinched joints depends on geometrical characteristics (the undercut and the neck thickness) that depends on the material flow. Thus, to improve the strength of those joints, different approaches are potentially suitable including the optimization of the tools sets, as well as the development of a two-steps clinching that involves a reshaping step after clinching. The latter method has been initially proposed to reduce the protrusion height (and thus to improve the aesthetical characteristics of such joints) [40]. However, further researches have demonstrated that two-steps clinching can also improve the mechanical strength of clinched joints made on aluminum sheets [41]. This results from the increase in neck thickness and undercut [24]. So far, any investigation has been performed to determine the influence of a reshaping step while joining by clinching metal with composite sheets, in terms of material flow, damage of the composite, characteristic dimensions and strength.

The present investigation analyzes two-steps clinching based on reshaping deformation that follows mechanical clinching, as a method to improve the mechanical behavior of clinched connections performed on hybrid metal-composites joints. In particular, aluminum alloy series AA6xxx and Carbon Fiber Reinforced Polymer (CFRP) sheets with long fibers and thermosetting matrix were joined by clinching. Different types of reshaping tools and values of joining forces were tested in order to determine the optimal process window. Mechanical tests based on single lap shear tests were performed to characterize the mechanical behavior of the joints and to verify the effectiveness of the reshaping method. In addition, morphological analysis was conducted to understand how the reshaping step influences the mechanical behavior, the main joints dimensions and the damage on CFRP sheet.

2. Materials and Methods

2.1 Materials

Rolled sheets of 3.0 mm thick aluminum alloy AA6024 were used in this study. This is a precipitation hardenable aluminum alloy with Si and Mg as the main alloying elements. The chemical composition of the aluminum was determined by means of a X-ray fluorescence spectrometer. The main chemical elements of the alloy are reported in Table 1. The aluminum sheet was coupled with a CFRP sheet with a thickness of 1.4 mm. The CFRP laminates were manufactured using plain weave (SK Chemical,UGN200). The carbon fiber prepregs (MRC PYROFILTM, TR30S) and a thermosetting epoxy resin (bisphenol-A type epoxy+phenol Novolac type epoxy) were cured for 2 h at 130 °C. The initial thickness of prepreg for a plywas 0.3mm before the pressure was applied. The final resin content was estimated to be about 53%, as reported in Table 2. The mechanical properties and fabrication procedure of the CFRP sheet are reported in [39]. The main characteristics and mechanical properties of the CFRP are reported in Table 2 and Table 3.

Table 1 Chemical composition of aluminum alloy.

Element	Mg	Si	Mn	Al
Concentration [%]	0.33	0.96	0.87	96.62

Table 2 Manufacturing conditions of CFRP

Type of woven fabric	Thickness of laminate [mm]	Number of plies	Fiber volume fraction [%]	Lay-up angle [deg]
Plain weave (3K)	1.4	7	53.3 ± 0.45	0

Table 3 Mechanical properties of CFRP and AA6082-T6 alloy

Material	Elastic modulus [GPa]	Yield Strength, $\sigma_{0.2}$ [MPa]	Ultimate tensile Strength [MPa]	Flow stress [MPa]	Bearing Strength [MPa]	ILSS [MPa]
AA6024	69	282	380	$\sigma_p = 459\varepsilon^{0.088}$	–	–
CFRP	175.3	-	962.7	–	366	19.1

2.2 Clinching equipment

Clinched tests were carried out by means of a portable clinching machine model Python by Jurado srl (Rivotorto (Perugia), Italy). In this investigation, the clinching configuration used in the first step was kept unchanged. In this step (mechanical clinching), a split die with three sectors, die anvil depth h=1.1 mm and initial diameter D=5.2 mm was used, as schematically depicted in Fig. 1(a). The split die was preferred to fixed (grooved) one because it generally produces larger undercuts with lower forming forces and it enables an easier extraction of composite crumbles from the die cavity [42]. The tool set of the first step also included a punch with taper angle of 6°, diameter d=4 mm and fillet radius of 0.2 mm. After performing the first joining step, the clinching tools were substituted and the second step was performed. In the second step (reshaping), the height of the punch was varied in order to produce different punch-die cavity geometries (reshaping depth, R_d). This was done by changing the height H_R of an adjustable ring, as depicted in Fig. 1(b). The study also investigated the effect of the reshaping force in the second step, which was varied over two levels F_j=20.5 kN and F_j=28.8 kN, while the forming force in the first step kept unchanged (F_j=28.8 kN). These values were selected according to preliminary test results and the maximum available force of the clinching machine. The experimental plan is summarized in Table 4. In all the tests, the aluminum was placed at the punch side.

Table 4 Experimental plan

Case	Reshaping depth, R_d [mm]	Reshaping force, F_j [kN]
NO	(No Reshape)	-
P20R$_d$2	2	20.5
P28R$_d$2	2	28.8
P20R$_d$1	1	20.5
P28R$_d$2	1	28.8
P20R$_d$0.5	0.5	20.5
P28R$_d$0.5	0.5	28.8

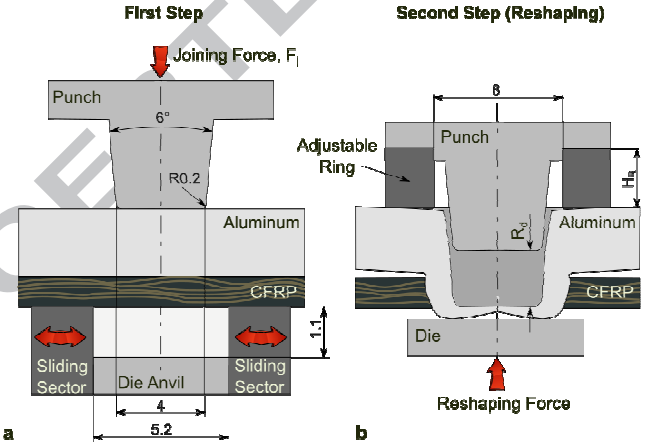

Fig. 1 Schematic of the adopted clinching tools in (a) first step and (b) second step.

2.3 Mechanical characterization of the joints

The mechanical behavior of the joints was assessed by means of single lap shear tests. To this end, a Universal Test machine model 322.31 by MTS was used using 25 kN full-scale under quasi-static conditions (constant crosshead speed 1 mm/min). The geometry and specimen dimensions are reported in Fig. 2a. For each joining condition, five replicates were performed and the average and standard deviation of the ultimate lap shear force F_r (maximum load recorded during the shear test) and absorbed energy W, calculated as the area underlying the load-displacement curve of a shear test, were determined.

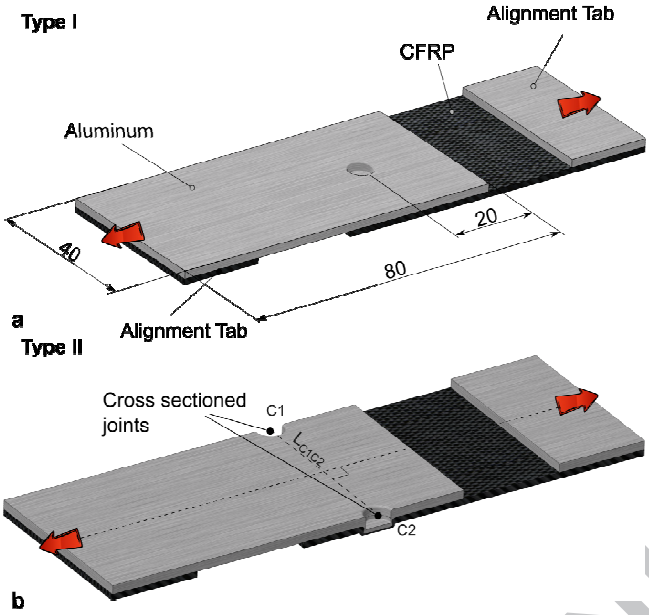

Fig. 2 Schematic of the specimens used for characterization tests: (a) single lap shear test and (b) "two halves" specimen used for analysis of material flow of cross-section.

To examine the deformation of the joint and crack propagation throughout the CFRP sheet during the single lap shear tests, a double-halves joint specimen (Type II) was adopted, as schematized in Fig. 2b. This specimen is constituted by two-halves joints (which were sectioned after joining by clinching). When producing these specimens great care was paid in order to produce the cross sections parallel to the loading direction, and the line L_{C1C2}, which passes by the joints centers (C1 and C2), perpendicular to the loading direction, as schematized in Fig. 2b. Three replications were performed for specimens Type II to ensure replicability of these tests.

This shape constrained the rotation of the specimen around the joint during the shear test. The cross section evolution during the shear test was thus recorded using a 16-bit DSL camera model D5200 by Nikon with resolution of 6000×4000 mounted on a stereo microscope model Stemi DV4 by Zeiss.

2.4 Analysis of joints morphology

To investigate the influence of the aforementioned process parameters and particularly the difference between clinched and reshaped joints, the cross-sections for all the specimens were analyzed. The joints were cut in the middle by means of a low-speed saw with diamond blade. The cross sections were thus analyzed by means of optical metallographic microscope model DM5000 by Leica Microsystems and the above-mentioned stereoscope under reflective light. For each tool set, the main geometrical parameters, namely the undercut t_s, neck thickness t_n, and bulge height H depicted in Fig. 3, were measured.

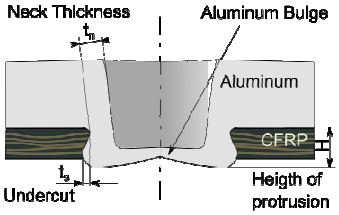

Fig. 3 Main geometrical characteristics of Aluminum/CFRP clinched joints.

3. Results and Discussion

3.1 Geometry of the joint

The cross-sections of the clinched joints made by single-step clinching (no reshape) and two-steps clinching are reported in Fig. 4. The cross sections of the joints show a certain asymmetry (different undercut and neck thickness values of the left and right hand sides of the joints). This is due to the high stiffness and anisotropy of the CFRP sheet that drives the aluminum material towards directions of less resistance (between fiber plies). To this end, five cross sections for each processing condition were analyzed.

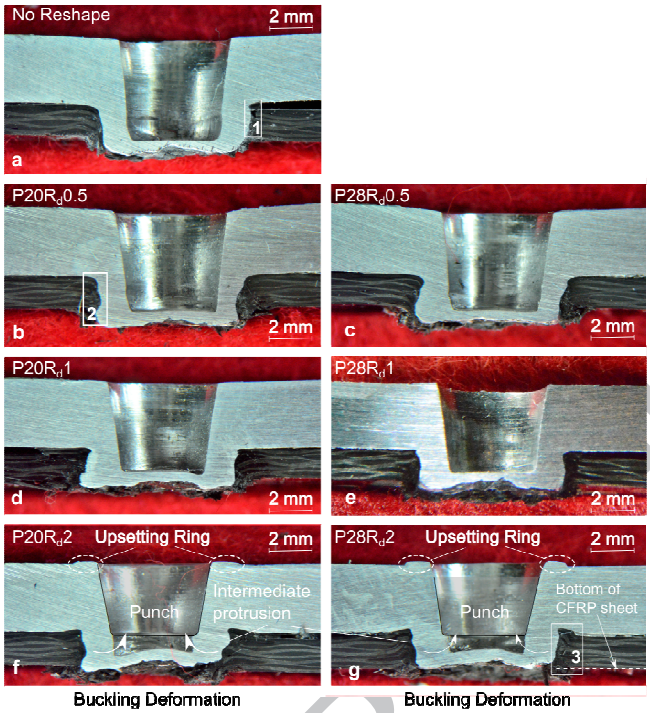

Fig. 4 Cross-sections of the joints produced under different processing conditions.

As can be observed from Fig. 4, no crack appear on the aluminum sheet at the neck region regardless the joining condition. Comparing the cross sections of "two-steps" joints with no-reshape ones, some differences can be appreciated. Indeed, the contact surface of aluminum-CFRP shown in Fig. 4a is relatively regular, while, on the other hand, by increasing the reshaping depth (R_d) the contact surface becomes more irregular showing intermediate side protrusions (as also depicted in Fig. 5b). In addition, excessive reshaping depths produced smaller contact surface (this was particularly evident in Fig. 4f-g and higher magnification reported in Fig. 5c) and bulge height (e.g. for P28R_d2 joints H=1.6±0.07 mm). This has potential detrimental effects of the mechanical behavior of the clinched joints as reported in [32]. In addition, when H is smaller than the thickness of the CFRP, the last plies of the CFRP hole are not in contact with the aluminum bulge promoting the onset of delamination and consequent reduction in load capacity.

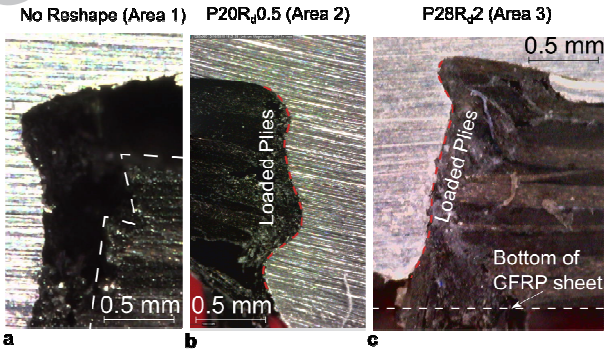

Fig. 5 Effect of reshaping on the contact between the aluminum bulge and CFRP hole by reshaping. The areas refer to selections depicted in Fig. 4.

The mechanical behavior of clinched joints is determined by several factors including the geometry of the joints, the length of contact arc, the bulge height, neck thickness and undercut dimensions [20], the damage that may develop during the joint formation [36] and strain hardening (since the process is generally carried out at room temperature) as well as the damage of the CFRP near the hole. To understand the influence of the reshaping tools on the mechanical behavior of the joints, the characteristic dimensions, namely the undercut t_s, neck thickness t_n were compared in Fig. 6.

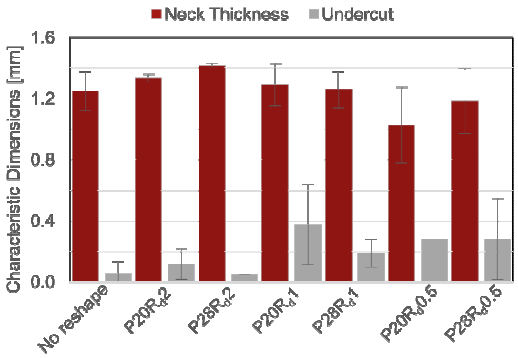

Fig. 6 Variation of the neck thickness and undercut by adopting different reshaping tools and joining forces.

Comparing the critical joint dimensions, it is evident that the undercut, which is much smaller than the neck thickness, represents the key parameter that determines the mechanical behavior of the joints.

The reshaping force is mainly exerted on the aluminum side-walls of the joint. Depending on the reshaping value R_d, this may result in different material flows. When small values of R_d are adopted, the reshaping step produces an increase in the undercut and higher contact pressure between the aluminum and CFRP (as also shown in the macrograph depicted in Fig. 5). When large values of R_d are used, the bulge height H reduces since the die pushes the aluminum bulge towards the joint axis rather than expanding the undercut, as shown in Fig. 5c.

3.2 Material flow

During the reshaping step, the aluminum side-wall is partially in contact with the punch (guided aluminum) as shown in Fig. 7, while the bottom part of the aluminum bulge is less constrained (free aluminum). When low values of R_d are adopted (e.g. R_d=0.5 mm), the free aluminum region is characterized by a reduced height; thus, this region is mainly subjected to upsetting that promotes an increase in the undercut and contact pressure between the aluminum and the surrounding CFRP, as schematized in Fig. 7a. On the other hand, when larger values of R_d are used (e.g. R_d=1.0 mm and R_d=2.0 mm) a different material flow is produced. Indeed, under such conditions, the greater height of the free aluminum region involves a lower stiffness. Thus, a higher instability is produced that promotes an inward bending of the aluminum bulge, which results in reduction of the undercut t_s and the bulge height H. The material flow produced under such conditions is schematized in Fig. 7b.

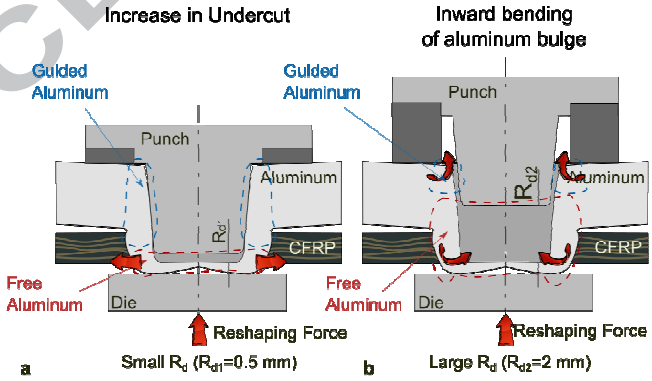

Fig. 7 Schematic of material flow using (a) small value of R_d and (b) large value of R_d.

When the higher levels of reshaping force were used, the material flow is accentuated: then, it resulted in higher increase in the undercut when R_d=0.5 mm and a higher reduction in the undercut for R_d=1.0 and 2.0 mm.

3.3 Mechanical behavior of the joints

Load-displacement curves of clinched joints made by different tools are reported in Fig. 8. All the joints failed by pull-out, which is a typical failure mode of clinched connections characterized by relatively small undercuts. The curves reported in Fig. 8 share a common behavior especially in the first path, which suggests that the stiffness of the joint is negligibly influenced by the reshaping step. On the other hand, the joints are characterized by different values of shear strength and absorbed energy, which demonstrates that the reshaping step can be positively employed to improve the mechanical behavior of clinched joints. Because of the pull-out failure mode, load-displacement curves shows a gradual load reduction after reaching the peak load (shear strength of the joint) up to the complete loss of the carrying load capability. This behavior is commonly preferable as compared to steeper load reduction trends (brittle behavior of the joint) as it enables more energy being absorbed by the joint, before the complete separation of the sheets.

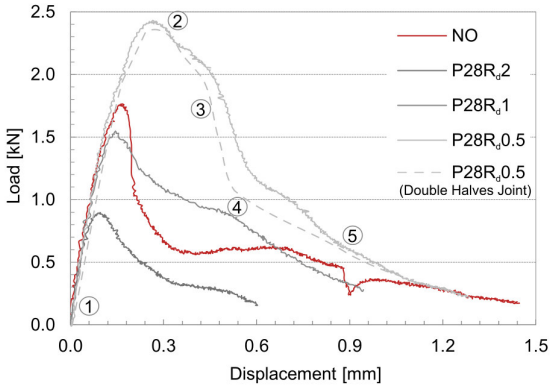

Fig. 8 Load-displacement curves of clinched joints made under different reshaping conditions and no reshape.

Fig. 9 depicts the evolution of the cross section (recorded by digital camera using the specimen of type II) for the highest strength specimen ($P28R_d0.5$). In the first phase of the shear test (almost linear path), the specimen undergoes a modest rotation (up to 1°), because of the relatively high thickness of the aluminum sheet. In addition, during this phase, any significant change in the joint cross section was observed (because of the large neck). However, as the peak load (shear strength of the joint) was reached, the CFRP showed greater damage, which resulted in load reduction. During this phase, the bearing load (exerted by the aluminum bulge) produced significant delamination and bucking in the CFRP hole, as shown in Fig. 8 (points 3-5).

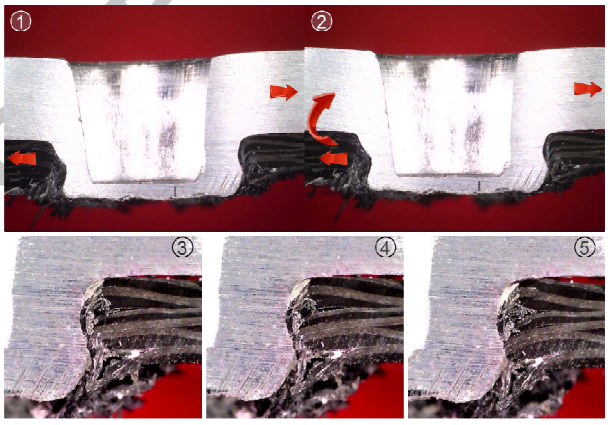

Fig. 9 Cross section of the clinched joint ($P28R_d0.5$) during the shear test.

Despites of the above-mentioned joint failure mode, different causes may compromise the mechanical performances of clinched joints due to the presence of defects and excessive damage of CFRP hole. Actually, the adoption of tools that produced an excessive reshaping depth reduction or excessive material flow resulted in premature onset of critical conditions that led to reduction of the shear strength and absorbed energy. Excessive material flow during the reshaping step, involved high damage in the composite hole (mainly

buckling and delamination). During the shear test, this also resulted in separation of the damaged CFRP (that adhered to the aluminum bulge) from the rest of the CFRP hole, as depicted in Fig. 10 a-d. Another type of defect, namely intermediate side protrusions was identified. This defect induced high concentration of contact loads, and produced early fractures in the CFRP with consequent reduction in load carrying capability Fig. 10e-h. Finally, tools involving high height reductions determined a smaller contact surface between the aluminum bulge and the CFRP hole. In this case, the last plies of the CFRP did not contribute to the load carrying during the shear tests, leading to a reduction of the mechanical strength of the joint.

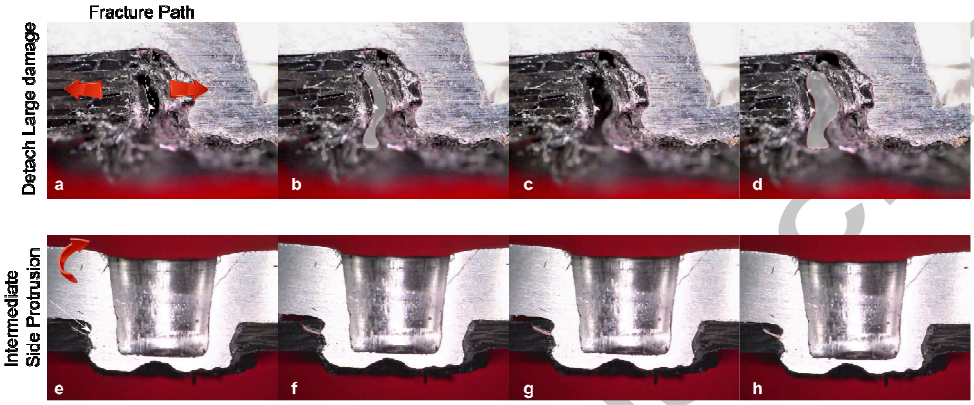

Fig. 10 Different fracture development: a-d Detach and e-h side protrusion fracture induced.

Fig. 11 compares the (a) shear strength and (b) absorbed energy of the joints made under different processing conditions. As can be inferred, the geometry of the tools used in the second step (reshape) had a stronger influence on the mechanical behavior of the joints as compared to the reshaping force.

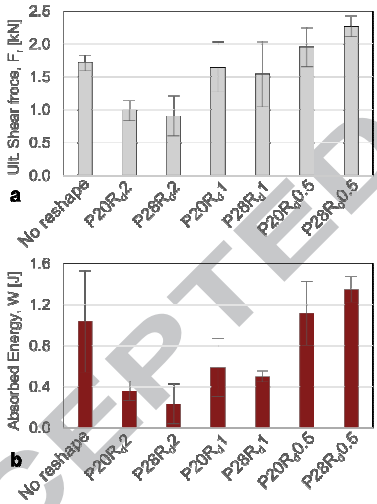

Fig. 11 Effect of reshaping tools and reshaping force on (a) ultimate shear force and (b) absorbed energy of the joints.

The reshaping tool with R_d=0.5 mm enabled an increase in the shear strength and the absorbed energy by 32% and 30%, respectively, as compared to the joints made without reshaping, since deformation schematically depicted in Fig. 7a w(increase in undercut) was promoted. On the other hand, higher reshaping depths (R_d=1 mm and R_d=2 mm) had detrimental effects on the mechanical properties of the joints, since deformation depicted in Fig. 7b (inward bending of the aluminum bulge) was induced. For R_d=0.5 mm, increasing the reshaping force yielded to higher strength and absorbed energy of the joints, while for R_d=1.0 mm and R_d=2.0 mm higher reshaping force resulted in a slight or higher reduction of both F_r and W. Therefore, the shape of the joining tools (reshaping depth) determined the direction of the material flow (increase in undercut or inward bending of the aluminum bulge) while the reshaping force determined the magnitude of the material flow.

3.4 Bearing Strength of the joints

The bearing strength of the clinched joints performed with and without the second (reshaping) step was compared with the bearing strength of the CFRP composite material, which was characterized by standard

bearing tests according to ASTM D5961-04 [43] standards [39]. To this end, the maximum bearing strength of the joints was calculated as the ratio of the ultimate shear force (recorded in single lap shear tests) by the CFRP resistance area A_b, schematized in Fig. 12 (given by the height of the composite material multiplied by the hole diameter).

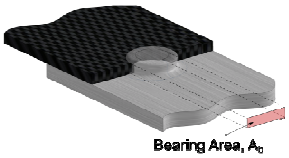

Fig. 12 Schematic of the resistance area A_b used for calculation of bearing strength of the joints.

Thus, to evaluate the bearing strength, the hole diameter of all the joints was measured. It was found that, the hole diameter was slightly influenced by the reshaping conditions (the diameter of all the joints ranged between 6.5 mm and 6.65 mm). Thus, the bearing strength of the joint followed a similar trend of that of the ultimate shear strength with the reshaping conditions. The joint made without the reshaping step was characterized by a bearing strength of 172 MPa while that made by the second step with R_d=0.5 mm and reshaping force of 28.8 kN showed a bearing strength of 227 MPa that is an increase by 32%. Such values are still lower than the bearing strength of the composite material (366 MPa) leading to a joint efficiency, calculated as the ratio of the joint strength by the CFRP bearing strength) of 62%.

4. Conclusions

The present investigation was aimed at verifying the suitability of mechanical clinching for producing hybrid CFRP–aluminum joints using extensible dies. Different geometries of the clinching tools were tested by varying the reshaping tools geometry while keeping the pin diameter and the taper angle unchanged. Geometrical and morphological analysis revealed the influence of the punch geometry and damage on the clinched joints. Single lap shear tests were carried out to assess the mechanical behavior of the joints. In addition, a new type of specimen consisting of a doubled-halves joint was developed to enable the observation of the clinched joint behavior during the shear test. The main findings of the research are as follows:

- The reshaping step is feasible for improving the mechanical behavior of such clinched connections; indeed, under optimal conditions it allowed to increase the shear strength and the absorbed energy by 32% and 30%, respectively as compared to no reshaped joints;
- The increase in the mechanical behavior was due to the increase in undercut (the joints failed by pull-out); in addition, a significant increase in the neck thickness was also observed;
- The geometry of the reshaping tools represents a critical parameter; actually, improper design of the tools may have detrimental effects on the geometry and consequently the mechanical properties of the clinched joint. Indeed when large values of the reshaping depth are used, the second step involves an inward-bending of the aluminum bulge that tends to reduce the undercut;
- The reshaping step increases the contact between the aluminum and the CFRP hole. However, excessive values of the reshaping depth yielded higher damage in the CFRP sheet due to buckling and delamination.
- The main defects appearing on the joints and their causes were identified.
- the bearing stress of the reshaped joints made under optimal conditions (227 MPa) also increased by 32% as compared to the joints made without the reshaping step (172 MPa).

Acknowledgements

The authors would like to thank Jurado (Rivotorto di Assisi, Italy) for providing the extensible dies used in this research. The authors would also like to thank Mr. Giuseppe Organtini (DIIIE - University of L'Aquila) for the contribute during the setup and conduction of the experimental tests. This work was also supported by the National Research Foundation of Korea (NRF) Grant funded by the Korean government (MSIP) (No.2012R1A5A1048294).

References

[1] Zhou Y, Fan H, Jiang K, Gou M, Li N, Zhu P, et al. Experimental flexural behaviors of CFRP strengthened aluminum beams. Composite Structures. 2014;116:761-71.
[2] Meng F, Li W, Fan H, Zhou Y. A nonlinear theory for CFRP strengthened aluminum beam. Composite Structures. 2015;131:574-7.
[3] Harries KA, Peck AJ, Abraham EJ. Enhancing stability of structural steel sections using FRP. Thin-Walled Structures. 2009;47:1092-101.
[4] Christke S, Gibson AG, Grigoriou K, Mouritz AP. Multi-layer polymer metal laminates for the fire protection of lightweight structures. Materials & Design. 2016;97:349-56.
[5] Zhou Y, Jiang K, Gou M, Li N, Zhu P, Wang D, et al. Prediction of debonding strength of tensile hybrid bonded joints using fracture mechanics. Materials & Design. 2014;61:87-100.
[6] Anyfantis KN, Tsouvalis NG. Loading and fracture response of CFRP-to-steel adhesively bonded joints with thick adherents – Part I: Experiments. Composite Structures. 2013;96:850-7.
[7] Medlin HKaD. ASM Handbook Volume 8: Mechanical Testing and Evaluation: ASM International; 2000.
[8] Kweon J-H, Jung J-W, Kim T-H, Choi J-H, Kim D-H. Failure of carbon composite-to-aluminum joints with combined mechanical fastening and adhesive bonding. Composite Structures. 2006;75:192-8.
[9] Matsuzaki R, Shibata M, Todoroki A. Improving performance of GFRP/aluminum single lap joints using bolted/co-cured hybrid method. Composites Part A: Applied Science and Manufacturing. 2008;39:154-63.
[10] Kashaev N, Ventzke V, Riekehr S, Dorn F, Horstmann M. Assessment of alternative joining techniques for Ti–6Al–4V/CFRP hybrid joints regarding tensile and fatigue strength. Materials & Design. 2015;81:73-81.
[11] Pickin CG, Young K, Tuersley I. Joining of lightweight sandwich sheets to aluminium using self-pierce riveting. Materials & Design. 2007;28:2361-5.
[12] Goushegir SM, dos Santos JF, Amancio-Filho ST. Friction Spot Joining of aluminum AA2024/carbon-fiber reinforced poly(phenylene sulfide) composite single lap joints: Microstructure and mechanical performance. Materials & Design. 2014;54:196-206.
[13] Liu FC, Liao J, Nakata K. Joining of metal to plastic using friction lap welding. Materials & Design. 2014;54:236-44.
[14] Balle F, Huxhold S, Wagner G, Eifler D. Damage Monitoring of Ultrasonically Welded Aluminum/ CFRP-Joints by Electrical Resistance Measurements. Procedia Engineering. 2011;10:433-8.
[15] Jung KW, Kawahito Y, Takahashi M, Katayama S. Laser direct joining of carbon fiber reinforced plastic to zinc-coated steel. Materials & Design. 2013;47:179-88.
[16] Abibe AB, Sônego M, dos Santos JF, Canto LB, Amancio-Filho ST. On the feasibility of a friction-based staking joining method for polymer–metal hybrid structures. Materials & Design. 2016;92:632-42.
[17] Park HS, Nguyen TT. Development of infrared staking process for an automotive part. IOP Conference Series: Materials Science and Engineering. 2015;95:012019.
[18] Blaga L, Bancilă R, dos Santos JF, Amancio-Filho ST. Friction Riveting of glass–fibre-reinforced polyetherimide composite and titanium grade 2 hybrid joints. Materials & Design. 2013;50:825-9.
[19] Seidlitz H, Ulke-Winter L, Kroll L. New Joining Technology for Optimized Metal/Composite Assemblies. Journal of Engineering. 2014;2014:1-11.
[20] Mucha J. The analysis of lock forming mechanism in the clinching joint. Materials & Design. 2011;32:4943-54.
[21] Mucha J, Witkowski W. The experimental analysis of the double joint type change effect on the joint destruction process in uniaxial shearing test. Thin-Walled Structures. 2013;66:39-49.
[22] Coppieters S, Lava P, Hecke RV, Cooreman S, Sol H, Houtte PV, et al. Numerical and experimental study of the multi-axial quasi-static strength of clinched connections. International Journal of Material Forming. 2012;6:437-51.
[23] Coppieters S, Lava P, Baes S, Sol H, Van Houtte P, Debruyne D. Analytical method to predict the pull-out strength of clinched connections. Thin-Walled Structures. 2012;52:42-52.

[24] Chen C, Zhao S, Han X, Cui M, Fan S. Investigation of the height-reducing method for clinched joint with AL5052 and AL6061. The International Journal of Advanced Manufacturing Technology. 2016.
[25] Chen C, Zhao S, Cui M, Han X, Fan S. Mechanical properties of the two-steps clinched joint with a clinch-rivet. Journal of Materials Processing Technology. 2016;237:361-70.
[26] Chen C, Zhao S, Cui M, Han X, Ben N. Numerical and experimental investigations of the reshaped joints with and without a rivet. The International Journal of Advanced Manufacturing Technology. 2016.
[27] Mucha J. The failure mechanics analysis of the solid self-piercing riveting joints. Engineering Failure Analysis. 2015;47:77-88.
[28] Mucha J. The numerical analysis of the effect of the joining process parameters on self-piercing riveting using the solid rivet. Archives of Civil and Mechanical Engineering. 2013.
[29] Mucha J. The effect of material properties and joining process parameters on behavior of self-pierce riveting joints made with the solid rivet. Materials & Design. 2013;52:932-46.
[30] He X, Liu F, Xing B, Yang H, Wang Y, Gu F, et al. Numerical and experimental investigations of extensible die clinching. The International Journal of Advanced Manufacturing Technology. 2014;74:1229-36.
[31] He X, Xing B, Zeng K, Gu F, Ball A. Numerical and experimental investigations of self-piercing riveting. The International Journal of Advanced Manufacturing Technology. 2013;69:715-21.
[32] Lambiase F. Mechanical behaviour of polymer-metal hybrid joints produced by clinching using different tools. Materials & Design. 2015;87:606-18.
[33] Lüder S, Härtel S, Binotsch C, Awiszus B. Influence of the moisture content on flat-clinch connection of wood materials and aluminium. Journal of Materials Processing Technology. 2014;214:2069-74.
[34] Behrens B-A, Rolfes R, Vucetic M, Peshekhodov I, Reinoso J, Vogler M, et al. Material characterization for FEA of the clinching process of short fiber reinforced thermoplastics with an aluminum sheet. 6th International Conference on Tribology in Manufacturing Processes & Joining by Plastic Deformation2014. p. 557-68
[35] Lambiase F, Durante M, Ilio AD. Fast joining of aluminum sheets with Glass Fiber Reinforced Polymer (GFRP) by mechanical clinching. Journal of Materials Processing Technology. 2016;236:241-51.
[36] Lambiase F, Di Ilio A. Damage analysis in mechanical clinching: Experimental and numerical study. Journal of Materials Processing Technology. 2016;230:109-20.
[37] Lee C-J, Lee J-M, Ryu H-Y, Lee K-H, Kim B-M, Ko D-C. Design of hole-clinching process for joining of dissimilar materials – Al6061-T4 alloy with DP780 steel, hot-pressed 22MnB5 steel, and carbon fiber reinforced plastic. Journal of Materials Processing Technology. 2014;214:2169-78.
[38] Lee S-H, Lee C-J, Lee K-H, Lee J-M, Kim B-M, Ko D-C. Influence of tool shape on hole clinching for carbon fiber-reinforced plastic and SPRC440. Advances in Mechanical Engineering. 2014;2014:1-12.
[39] Lambiase F, Ko D-C. Feasibility of mechanical clinching for joining aluminum AA6082-T6 and Carbon Fiber Reinforced Polymer sheets. Materials & Design. 2016;107:341-52.
[40] Wen T, Wang H, Yang C, Liu LT. On a reshaping method of clinched joints to reduce the protrusion height. The International Journal of Advanced Manufacturing Technology. 2014;71:1709-15.
[41] Chen C, Zhao S, Han X, Cui M, Fan S. Investigation of mechanical behavior of the reshaped joints realized with different reshaping forces. Thin-Walled Structures. 2016;107:266-73.
[42] Lambiase F, Di Ilio A. An experimental study on clinched joints realized with different dies. Thin-Walled Structures. 2014;85:71-80.
[43] ASTM D5961. Standard Test Method for Bearing Response of Polymer Matrix Composite Laminates. ASTM International, West Conshohocken, PA.; 2004.

List of Figure Captions

List of Table Captions